



Quercitrin: a New Immunosuppressant Inhibits Calcineurin*

WANG Meng-Qi^{1,2)**}, LIU Ji-Qiong^{1)**}, TONG Li^{1)**}, XIE Yu-Fei^{1,3)}, CHEN Hui¹⁾,
ZHAO Chang-Yun¹⁾, WANG Lei¹⁾, LIU Yuan-Yuan¹⁾, GAO Ya-Dan¹⁾, ZHANG Mu¹⁾,
XIANG Ben-Qiong^{1)***}, WEI Qun^{1)***}

(¹)Department of Biochemistry and Molecular Biology, Beijing Normal University, Gene Engineering and Biotechnology Beijing Key Laboratory, Beijing 100875, China;

(²)Beijing Normal University Publishing Group, Beijing 100088, China;

(³)School of Chemistry and Bioengineering, Changsha University of Science and Technology, Changsha 410114, China)

Abstract Objective This study aimed to search for immunosuppressants with high-efficiency and low-toxicity from Chinese herbal medicine using calcineurin (CN) as the target enzyme. **Methods** Natural compound which could inhibit the activity of the target enzyme, CN, was screened and one effective compound was identified and isolated. The immunosuppressive effect and toxic side effects of the compound were evaluated at the cellular and animal levels. The underlying immunosuppressive mechanism was explored using fluorescence spectroscopy, molecular docking, Western blot, dual-luciferase reporter gene, real-time PCR, etc. **Results** Quercitrin inhibited CN activity both *in vitro* and *in vivo*. In addition, it reduced the proliferation of splenocyte and ameliorated DTH symptoms in mice. Toxicological study showed that quercitrin had no or minimal toxic side effects on experimental animals. Fluorescence spectroscopy and molecular docking analysis showed that quercitrin may bind to two sites on the CN and regulate immune responses through the CN-NFAT pathway. **Conclusion** We identified a new CN inhibitor, quercitrin, which could be a useful novel immunosuppressant with low toxicity.

Key words quercitrin, calcineurin, immunity, CN-NFAT signal pathway, interaction

DOI: 10.16476/j.pibb.2021.0381

Immunosuppressive drugs are widely used in organ transplantation and autoimmune diseases. The discovery of cyclosporin A (CsA) and tacrolimus (FK506) in the 1980s opened up new avenues for organ transplantation and the treatment of autoimmune diseases^[1]. These agents reduced transplant rejection rates and improved patient survival^[2-3]. In 1991, Liu *et al.*^[4] reported that calcineurin was the target of both CsA and FK506.

Calcineurin (CN), is a unique calcium/calmodulin-dependent serine/threonine protein phosphatase; it is a heterodimer composed of a ~60 ku catalytic A subunit (CNA) and a ~19 ku regulatory B subunit (CNB)^[5]. CNA has one N-terminal catalytic domain and three regulatory domains, namely a CNB-binding domain (BBH), a CaM-binding domain (CBD) and an autoinhibitory domain (AID)^[6]. It is

involved in a host of critical physiological and pathological processes including muscle growth, T lymphocyte activation, apoptosis and cardiac hypertrophy^[5, 7]. CN controls T cell activation via the CN-nuclear factor of activated T cells (NFAT) pathway. In response to various triggers, calcium enters the T cell and binds to calmodulin, which then activates CN. The activated CN dephosphorylates NFAT, leading to its nuclear translocation and the

* This work was supported by a grant from The National Natural Science Foundation of China(30970636).

** These authors contributed equally to this work.

*** Corresponding author.

WEI Qun. Tel: 86-10-58807365, E-mail: weiq@bnu.edu.cn

XIANG Ben-Qiong. Tel: 86-10-58807221, E-mail: xiangbq@bnu.edu.cn

Received: December 8, 2021; Accepted: December 25, 2021

transcription of target genes, including cytokine genes such as IL-2 in human T cells, and the corresponding cytokines activate the immune response^[8-9]. CsA and FK506 combine with their specific cytoplasmic receptors (cyclophilin and FK506-binding protein (FKBP), respectively) to form complexes that bind to CN and inhibit the immune response^[1, 10].

Until now, CsA and FK506 remain the drugs of choice in the clinic^[11-12], but their dramatic side effects, including nephrotoxicity, neurotoxicity and hypertension^[12-14], limit their utility. These side effects of CsA and FK506 are particularly important since patients generally need to take the drugs for a long time. Therefore, effective CN inhibitors of low toxicity would be extremely desirable. In our laboratory we have established a mature system for screening inhibitors of CN, and have already identified several compounds^[15-17].

Chinese traditional herbal medicine is an important source of modern drugs. Many Chinese herbals have been evaluated as potential therapeutic agents. *Albizzia julibrissin* Durazz, also known as the Persian silk tree or pink siris, is a small domed or flat-topped, spreading tree with smooth, gray-brown bark and doubly pinnate leaves^[18]. The flowers of this plant are used to treat depression, insomnia, amnesia, sterility and obesity in oriental traditional medicine^[19-20], and immunity-related studies have also been reported^[21-22]. Using our screening system we identified a low toxicity flavonoid that inhibited calcineurin activity in *Albizzia julibrissin*. In initial work we showed that this compound was quercitrin, which has been reported to be an inhibitor of sortase A^[23], to have anti-inflammatory and anti-tumor activity via the NF-κB pathway^[24-25], and an excellent therapeutic effect in systemic lupus erythematosus (SLE)^[26] and imiquimod-induced psoriasis-like skin lesions murine model^[27].

To explore its immunomodulatory activity, we investigated its effect on the proliferation of ConA-stimulated murine spleen lymphocytes, LPS-stimulated murine spleen lymphocytes, the *in vitro* mixed lymphocyte reaction (MLR), and delayed type hypersensitivity (DTH). We also used fluorescence spectroscopy and molecular docking to examine the effects of quercitrin on CN and obtained preliminary evidence that quercitrin acts on the CN-NFAT signaling pathway *in vivo*.

1 Materials and methods

1.1 Ethics statement

All animal experimental procedures were authorized by the Ethics and Animal Welfare Committee, School of Life Science, Beijing Normal University (NO. CLS-EAW-2013-015) and were executed in strict accordance with United Kingdom Scientific Procedures Act (1986). All efforts were made to minimize the number of animals used and their suffering.

1.2 Materials

Flowers of *Albizzia julibrissin* Durazz were purchased from Beijing Tongrentang head store (Beijing, China). BL21 (DE3) strains harboring CNA cDNA and the cDNA for a deletion of CNA encoding the catalytic domain only were from our laboratory. BALB/c and C57BL/6 mice (6–8 weeks) were purchased from Vital River Laboratories (Beijing, China). Jurkat cells were obtained from the American Type Culture Collection. (FL)-NFAT plasmid and the p-renilla luciferase (RL)-SV40 plasmid were from our laboratory. The other reagents were all of standard laboratory grade.

1.3 Expression and purification of proteins

CNA and CNAa (catalytic domain only) were expressed and purified as described previously^[28]. Protein purity was assessed by SDS-PAGE. Protein concentrations were measured by the procedure of Bradford.

1.4 Extraction and isolation of compounds for screening

Air-dried flowers of *Albizzia julibrissin* Durazz was ground into a powder, then extracted with 70% ethanol. The concentrated extract was dispersed in water and partitioned successively with petroleum ether, ethyl acetate (EtOAc) and n-butanol. The EtOAc fraction was subjected to silica gel chromatography using trichloromethane and methanol (80 : 1–0 : 1, v/v) as solvent, to yield 7 fractions. The third fraction was subjected to polyamide column chromatography and high-speed countercurrent chromatography (HSCCC) and then recrystallized with methanol to yield the compound.

1.5 Compound identification

The compound was identified as quercitrin by ¹H NMR and ¹³C NMR analysis and comparison with the literature.

1.6 CN activity assays *in vitro*

Enzyme activity was measured using the method described in detail previously^[16]. Phosphatase activities are presented as percentages of control phosphate activity. Quercitrin stock solution was dissolved in DMSO. Assays using p-nitrophenyl phosphate (p-NPP) (Sigma-Aldrich, America) as substrate were monitored by spectrophotometer at 410 nm. When the substrate was ³²P-RII peptide (BioMoL Research Labs, America), the released ³²P was quantified by liquid scintillation spectrometry, and vehicle served as the matched control.

1.7 Cell viability assay

Cell viability was measured using the CCK-8 assay as described previously^[15]. Final concentrations of quercitrin were 2, 5, 10, 20, 50, 100, 500, 1 000 and 2 000 μmol/L, those of CsA (TCI, America) were 2, 5, 10, 20 and 50 μmol/L. The highest content of DMSO was 0.4%. Plates were incubated for 20, 44 and 68 h at 37°C in 5% CO₂, then 20 μl of CCK-8 (Dojindo, Japan) reagent was added to the wells and incubated for 4 h. The experiment was repeated five times. Cell viability was calculated from the following equation: Viability/% = (A_{450} of quercitrin group / A_{450} of control group) × 100.

1.8 Con A/LPS-induced mouse splenocyte proliferation

Splenocyte proliferation was measured as described^[15]. The final concentrations of quercitrin were 2, 10, 50, 100, 500 and 1 000 μmol/L. Proliferation was measured using the CCK-8 assay as described above. Cell growth inhibition was calculated from the following equation: Inhibition/% = [(A_{450} of control group - A_{450} of quercitrin group) / A_{450} of control group] × 100.

1.9 Mixed lymphocyte reaction (MLR)

A unidirectional MLR was performed with five replicates as previously described^[15]. The final concentrations of quercitrin were 0.1, 0.5, 2, 10, 50 and 100 μmol/L. The highest content of DMSO was 0.1%. After 48, 72 and 96 h of incubation, proliferation was measured using the CCK-8 assay.

1.10 Toxicity test

The acute toxicity test was performed in mice using the maximum amount of drug method together with the fixed-dose procedure, which is a sequential testing scheme proposed by the British Toxicology Society in 1984^[29]. Briefly, in the test the estimated

median lethal dose (LD_{50}) is used to assess the toxicity of the substance being investigated. If the LD_{50} is larger than 2 000 mg/kg of body mass, the substances will be termed “unclassified”. Sixteen mice, eight of each sex, were divided into two groups. Quercitrin was administered orally at a dose of 5 000 mg/kg to one group and intraperitoneally at a dose of 2 000 mg/kg to the other. Quercitrin dissolved in DMSO was diluted with a 0.5% aqueous solution of sodium carboxymethyl cellulose. The highest content of DMSO was 10%. The mice were observed for two weeks to assess any changes in reactivity, gait, motor activity, respiration rate, etc., and especially survival.

To further investigate the effect of quercitrin in animals, BALB/c mice were randomly divided into the following three groups (six per group): control group, CsA group and quercitrin group. Mice in the control group received an intraperitoneal injection of 0.2 ml 0.9% NaCl daily for 4 d, mice in the CsA group received the same volume containing 200 mg/kg CsA on the first day and 40 mg/kg on the following three days, and mice in the quercitrin group received the same volume containing 200 mg/kg quercitrin on the first day and 40 mg/kg on the following three days. CsA and quercitrin dissolved in 0.9% NaCl. Blood was taken and assays were performed to determine levels of glutamic-pyruvic transaminase, glutamic-oxalacetic transaminase, alkaline phosphatase, total bilirubin, urea nitrogen and serum creatinine.

1.11 Delayed type hypersensitivity (DTH) assay

DTH assay was carried out as previously described^[30]. Male BALB/c mice were randomly divided into the following five groups (eight per group): control group, CsA group, and three experimental quercitrin groups. Drugs were administered intraperitoneally to the appropriate groups for 5 d: the control group (0.9% NaCl), CsA group (40 mg/kg) and quercitrin groups (10, 20, 40 mg/kg).

1.12 Fluorescence quenching of proteins in the presence of quercitrin

Fluorescence measurements were made with a Fluoro Max-2 Fluorimeter (Jobin Yvon-Spex, France). Fluorescence emission spectra were recorded as described before^[31]. Molar ratios of drug to protein were 0, 1, 1.5, 2, 3, 4, 6, 8 and 12. Fluorescence

quenching was analyzed using a Stern-Volmer quenching plot^[32] (Equation (1)), as follows:

$$F_0/F = 1 + K_Q\tau_0[Q] = 1 + K_D[Q] \quad (1)$$

where F_0 and F are the fluorescence intensities in the absence and presence of quencher, respectively, $[Q]$ is the concentration of quencher, and K_D is the Stern-Volmer quenching constant, defined as $K_D = K_Q\tau_0$, where K_Q is the bimolecular quenching constant and τ_0 (assumed to be 10^{-8} s)^[33] is the lifetime of the fluorophore in the absence of quencher.

1.13 Docking

Docking experiments were carried out with Autodock 4.0. The macromolecule CN was treated as rigid, and quercitrin was treated as flexible. The first 35 docking results were compared with the potential binding areas from the fluorescence analysis. All figures were rendered using PyMOL.

1.14 CN activity assays of Jurkat cells

CN activity *in vivo* was determined using the assay described previously^[16]. Phosphatase activities are shown as percentages of control activity.

1.15 Western blot analysis of CN in Jurkat cells

Jurkat cells plated in 6-well plates were treated with 100 µg/L phorbol 12-myristate 13-acetate (PMA) (Sigma-Aldrich, America) and 1 µmol/L ionomycin (Ion) (Sigma-Aldrich, America). Cells received PMA and Ion or a combination of CsA or different doses of quercitrin and PMA and Ion. The cells were harvested by centrifugation after 24 h and washed twice with PBS. Then, they were lysed on ice for 15 min. Cell-free supernatants were collected for Western blot analysis. Protein quantitation was performed with a bicinchoninic acid (BCA) protein quantitation kit (Thermo Fisher Scientific, America). The samples were separated by discontinuous SDS-PAGE and transferred to PVDF membranes (Merck Millipore, America), which were blotted with primary antibodies (Cell Signaling Technology, America) and secondary antibodies, and specific bands were visualized using an electrochemiluminescence (ECL) kit (Engreen, China).

1.16 Dual-luciferase reporter gene assay

NFAT transcription activity was investigated using the two-reporter gene assay system. Jurkat cells plated in 24-well plates were cotransfected with the p-firefly luciferase (FL)-NFAT plasmid and the p-renilla luciferase-SV40 endogenous control plasmid. Twenty-four h after transfection, cells were

incubated with PMA + Ion or a combination of different doses of quercitrin and PMA + Ion for 24 h. NFAT activity was measured using a Dual-Luciferase Reporter Kit (Promega, America) according to the manufacturer's protocol.

1.17 Relative quantitative real-time PCR for IL-2

RNA was extracted from Jurkat cells using TRIzol reagent (Invitrogen, America). Relative quantitative real-time PCR was performed to detect the transcriptional level of IL-2. The primer sequences for IL-2 were TGTCACAAACAGTGCACCTACTTC (forward) and TGTGGCCTTCTGGGCATGT (reverse). For β-actin they were GTGACAGCAG-TCGGTTGGAG (forward), and AGTGGGGTGGC-TTTAGGAT (reverse). β-actin was used as an endogenous control gene. Real-time quantitative PCR was performed on an Applied Biosystems 7500 Real-Time PCR System using SYBR green dye. The reactions were performed in triplicate and the results are shown as $\bar{x} \pm s$.

1.18 Statistical analysis

The results are expressed as the mean±standard error of the mean. The GraphPad Prism 5.0 software was employed to calculate data and draw plots. Student *t* test was used to analyze the differences between groups, and significant were deemed at three levels: $P < 0.05$ (*), $P < 0.01$ (**), $P < 0.001$ (***/###).

2 Results

2.1 Expression and purification of CNA and its deletion mutant

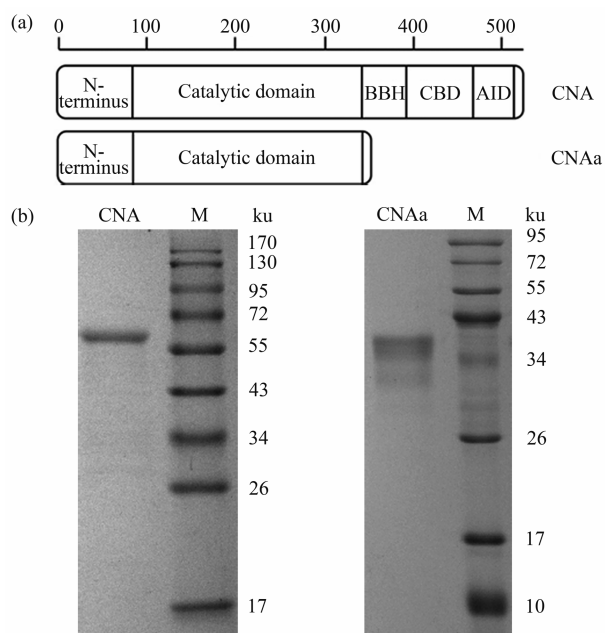
CNA and CNAa (Figure 1a) were expressed, purified in a series of steps and analyzed by SDS-PAGE (Figure 1b). Both were electrophoretically pure.

2.2 Identification of the screened flavonoid as quercitrin

We tracked the inhibitory activity of different fractions from *Albizia julibrissin* by CN activity assays. After continuous isolation and activity detection, we finally obtained a compound giving the strongest inhibition of CN.

The compound was a yellow amorphous powder, and the NMR data were as Table 1.

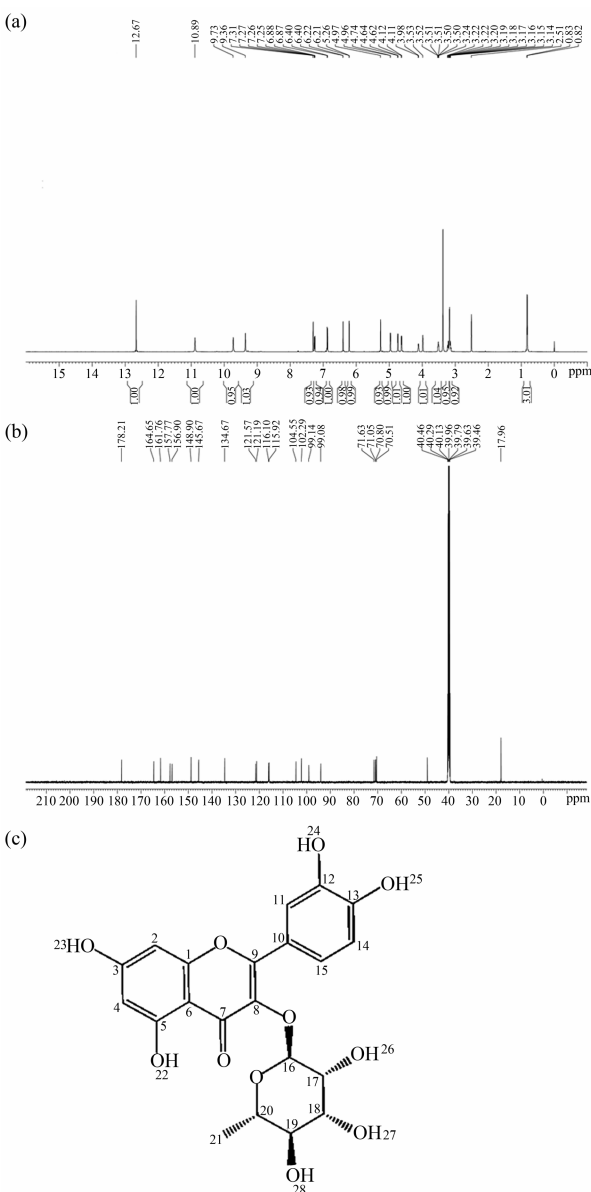
Comparison of the compound's ¹H NMR and ¹³C NMR spectra with those reported in the literature^[34], allowed us to identify it as quercitrin, purity>95% (Figure 2).

**Fig. 1 Characterization of proteins**

- (a) Schematic representation of CNA and its truncated derivatives.
 (b) SDS-PAGE analysis of purified CNA and CNaa.

Table 1 ^1H (500 MHz) and ^{13}C (125 MHz) NMR assignments of quercitrin in DMSO- d_6

No.	δ_{H} (J / Hz)	δ_{C}
1		157.8
2	6.40, d (1.8)	94.1
3		164.6
4	6.21, d (1.8)	99.1
5		161.8
6		102.3
7		178.2
8		134.7
9		156.9
10		121.6
11	6.87, d (8.3)	115.9
12		145.7
13		148.9
14	7.26, dd (8.3, 1.8)	116.1
15	7.308, d (1.8)	121.2
16	5.26, s	104.5
17	3.98, brs	71.6
18	3.54–3.48, m	70.5
19	3.16–3.12, m	71.1
20	3.25–3.19, m	70.8
21	0.82, d (6.0)	18.0
22	12.67, s	
23	10.89, s	
24	9.73, s	
25	9.36, s	
26	4.96, d (4.3)	
27	4.74, d (4.6)	
28	4.63, d (5.7)	

**Fig. 2 Compound identification**

- (a) ^1H NMR spectrogram of compound. (b) ^{13}C NMR spectrogram of compound. (c) Chemical structure of quercitrin.

2.3 Quercitrin inhibits CN activity *in vitro*

Quercitrin inhibits CN activity *in vitro* with either p-NPP or ^{32}P -RII peptide as substrate. IC_{50} values were 1.59 mmol/L (p-NPP, Figure 3a) and 22.59 $\mu\text{mol/L}$ (^{32}P -RII peptide, Figure 3b), respectively. The effects of quercitrin were strikingly different from those of CsA and FK506, which inhibit CN activity with RII as substrate but stimulate CN activity with p-NPP as substrate^[35].

2.4 Inhibition of Con A or LPS-induced proliferation and the MLR by quercitrin

The cytotoxic effect of quercitrin on mice spleen cells measured over 24, 48 and 72 h by CCK-8 assay,

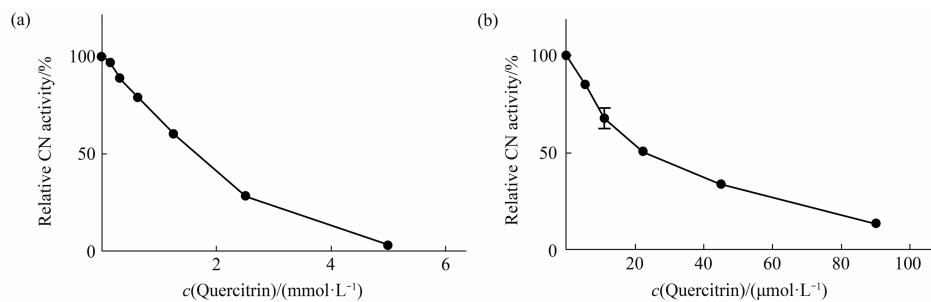


Fig. 3 Inhibition of CN activity *in vitro* by quercitrin

(a) Phosphatase activity measured with p-NPP as substrate. (b) ^{32}P -RRI peptide as substrate. CN activity is shown as a percentage of that in the control group. All values are expressed as $\bar{x} \pm s$. $n = 4$.

was lower than that of CsA. The IC_{50} values of CsA were 18.85 $\mu\text{mol/L}$ (24 h), 8.82 $\mu\text{mol/L}$ (48 h) and 4.86 $\mu\text{mol/L}$ (72 h). Quercitrin only had a weak inhibitory effect on growth of the cells at concentrations equal to or above 500 $\mu\text{mol/L}$.

To evaluate the immunosuppressive effects of

quercitrin, we used Con A or LPS-stimulated proliferation assays and the MLR assay. Quercitrin inhibited the growth of T lymphocytes, B lymphocytes and one-way mixed lymphocytes (Figure 4a–c), and inhibition was time- and dose-dependent.

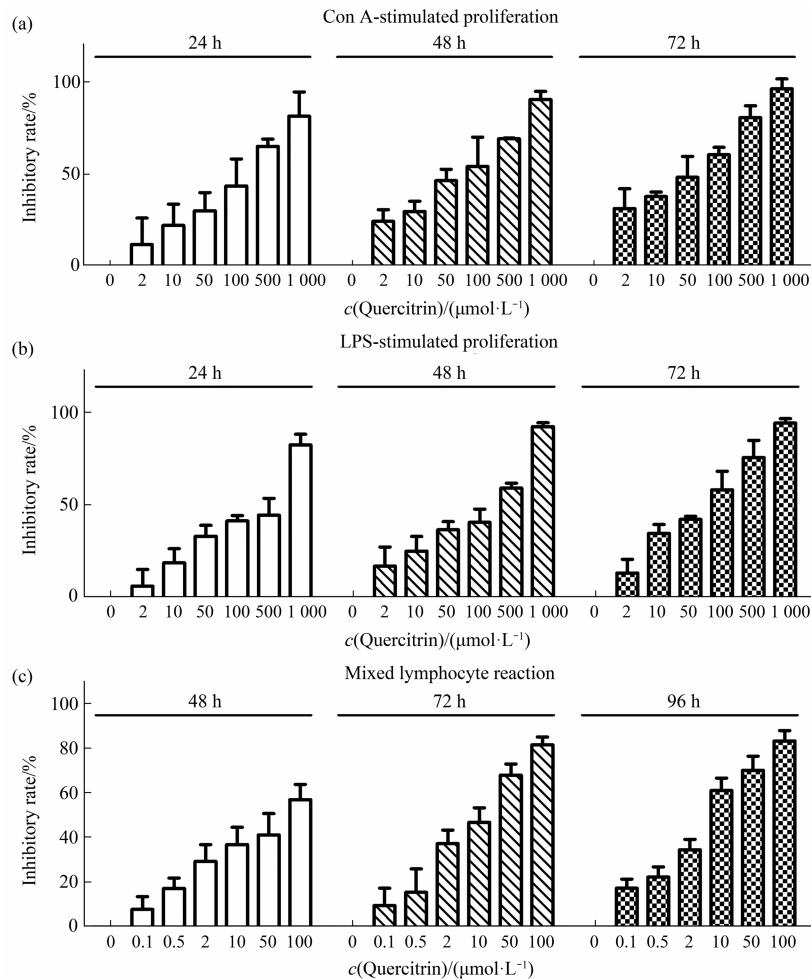


Fig. 4 Inhibition of Con A or LPS-stimulated proliferation and MLR by quercitrin

(a) Effect of different concentrations of quercitrin on Con A-induced lymphocyte proliferation. (b) Effect of different concentrations of quercitrin on LPS-induced lymphocyte proliferation. (c) Effect of different concentrations of quercitrin on MLR. Assessed by CCK-8 assay for 24, 48, 72 and 96 h. Results are expressed as $\bar{x} \pm s$. $n = 5$ for each group.

2.5 Quercitrin is non-toxic and has no significant hepatotoxicity and nephrotoxicity in mice

Mice treated with quercitrin (2 000 mg/kg, *i. p.* and 5 000 mg/kg, *i. g.*) were fully observed for 14 d (twice daily). The mice exhibited some degree of malaise in the initial half hour, and then returned to normal. There were no toxic reactions, deaths or obvious weight changes over 14 d. On day 14, the mice were killed and dissected to observe their organs; there were no visible lesions. Substances estimated with an indicating that quercitrin can be identified as “unclassified”.

In order to further study the effect of quercitrin on the activities of the mouse kidney and liver, three groups of mice (control, CsA and quercitrin), after treatment with the respective drugs for four d, were used to provide sera for blood biochemistry analysis. From Figure 5, it can be seen that quercitrin was less toxic than CsA at equivalent doses.

2.6 Quercitrin alleviates paw edema in DTH mice

The DTH assay was employed to evaluate the impact of quercitrin on immunoregulation. The results are shown in Table 2. Low doses of quercitrin had no significant effect on the paw edema. However, high doses of quercitrin and CsA alleviated the paw edemas in the DTH mice. Quercitrin had a similar effect on spleen cell numbers in the DTH mice (Table 2).

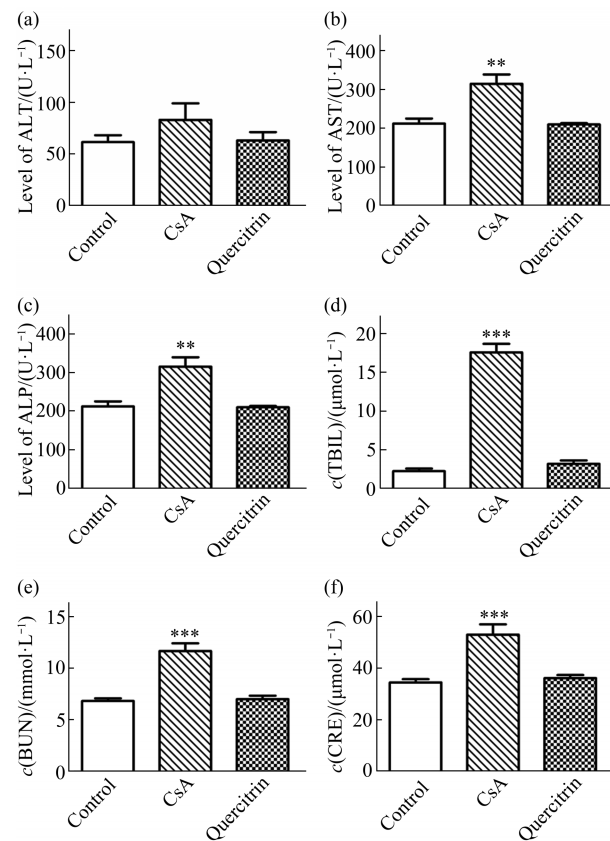


Fig. 5 Toxicity of quercitrin in mice

Biochemical tests on sera of control BALB/c mice and mice treated with CsA or quercitrin. $n=6$ for each group. Dosage schedule: 200 mg/kg on day 0, 40 mg/kg on days 1, 2 and 3; blood sampling on day 4. (a) Glutamic-pyruvic transaminase (ALT). (b) Glutamic-oxalacetic transaminase (AST). (c) Alkaline phosphatase (ALP). (d) Total bilirubin (TBIL). (e) Urea nitrogen (BUN). (f) Serum creatinine (CRE). Bars represent $\bar{x} \pm s$ from 6 mice. ** $P < 0.01$ and *** $P < 0.001$ for comparison with control group.

Table 2 Percentage inhibition of paw swelling by quercitrin and CsA in DTH ($n=8$)

Treatment	Dose/(mg·kg ⁻¹)	Paw swelling/mm	Percentage inhibition	Spleen cells/ 10^7	Percentage of spleen cells/%
Control	0	0.72±0.10	—	7.65±0.13	100
Quercitrin	10	0.69±0.08	4.17%	6.95±0.30	90.8
	20	0.49±0.10***	31.94%	6.14±0.19***	80.3
	40	0.28±0.07***	61.11%	5.44±0.13***	71.1
CsA	40	0.23±0.02***	68.06%	5.28±0.12***	69

*** $P < 0.001$.

2.7 Quercitrin reduces CN activity, not expression, in cells

We investigated quercitrin inhibition of CN activity *in vitro* using Jurkat cells, human T cell leukaemia cells. The Jurkat cells were cultured in 6-well plates and treated with quercitrin for 24 h. Inhibition of CN activity by quercitrin was dose-dependent, and the IC_{50} value was 107.54 $\mu\text{mol/L}$ (Figure 6a).

We also assessed the effect of quercitrin on CN expression in Jurkat cells. Figure 6b shows that

quercitrin had no effect on the expression of CN.

2.8 Quercitrin inhibits of NFAT activity and IL-2 transcription

CsA, a classical CN inhibitor, exerts its immunosuppressive effect by inhibiting the CN-NFAT pathway, and IL-2 is one of the NFAT target genes. To test whether quercitrin also acted on this signaling pathway, we measured the effect of quercitrin on NFAT activity and IL-2 transcript levels. As shown in Figure 6c and 6d, quercitrin inhibited both NFAT and IL-2 transcription in a dose-dependent manner.

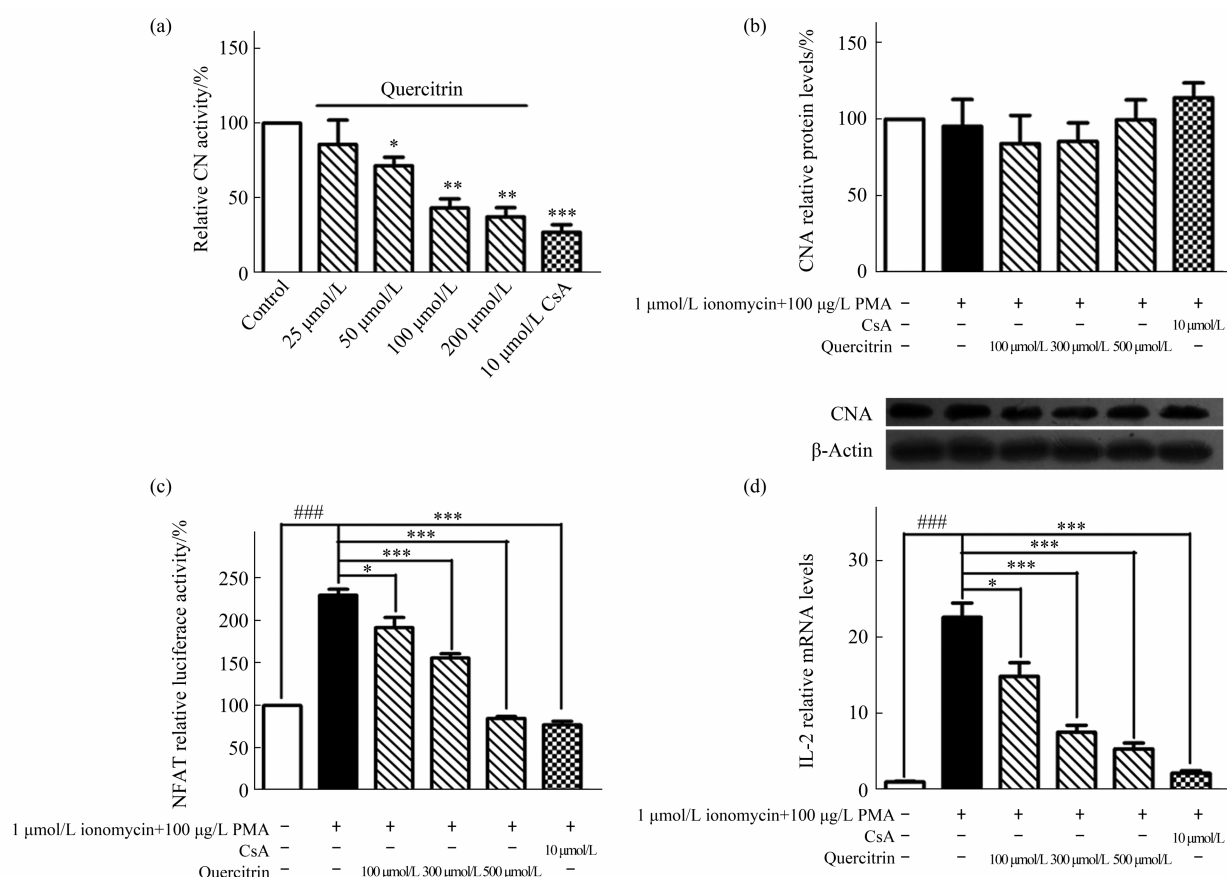


Fig. 6 Effect of quercitrin in Jurkat cells

(a) Quercitrin inhibits CN activity *in vivo*. (b,c) Cells were stimulated with PMA + Ion or a combination of indicated concentrations quercitrin or CsA and PMA + Ion for 24 h; Effect of quercitrin on CN expression (b) and effect of quercitrin on NFAT activity measured by dual-reporter gene assay system (c). (d) Cells were stimulated with PMA + Ion for 6 h or a combination of indicated concentrations quercitrin or CsA for 18 h and added PMA + Ion for another 6 h. Effect of quercitrin on IL-2 mRNA expression assayed by real-time PCR. All data are expressed as $\bar{x} \pm s$. $n = 3$. *** $P < 0.001$ for comparison with blank, * $P < 0.05$, ** $P < 0.01$ and *** $P < 0.001$ for comparison with control group.

2.9 Fluorescence quenching of CNA and its deletion mutant by quercitrin

First, we confirmed that 2% DMSO did not alter the basic shape of the emission spectrum of CNA,

then examined the effect of quercitrin. Figure 7a shows that the fluorescence of CNA was gradually quenched as the concentration of quercitrin increased, and there was a slight blue shift of the maximum emission wavelength in the presence of quercitrin. We

plotted regression curves according to Equation (1), (Figure 7b) and calculated a K_Q of $(1.32 \pm 0.37) \times 10^{13} \text{ L} \cdot \text{mol}^{-1} \cdot \text{s}^{-1}$ ($n=3$, relative coefficient $R > 0.99$), This was greater than $2 \times 10^{10} \text{ L} \cdot \text{mol}^{-1} \cdot \text{s}^{-1}$ implying that a static quenching mechanism was operative; in other words, quercitrin and CNA form a complex that results in quenching of the fluorescence. We then plotted a regression line based on Equation (2) (Figure 7c), and calculated a K_A of $(1.60 \pm 0.40) \times 10^6 \text{ L} \cdot \text{mol}^{-1}$ with a number of binding sites n of (1.17 ± 0.07) ($R > 0.99$). These data show that quercitrin binds to CN with a stoichiometry of 1 : 1, and the binding intensity is quite strong.

$$\lg [(F_0 - F) / F] = \lg K_A + n \lg [Q] \quad (2)$$

In order to explore more accurately the binding region between quercitrin and CNA, we used

fluorescence spectroscopy to study the interaction between quercitrin and CNAa. As Figure 7d shows, the fluorescence of CNAa also gradually declined as the concentration of quercitrin increased. We plotted regression curves according to Equation (1) (Figure 7e) and calculated K_Q to be $(1.71 \pm 0.24) \times 10^{13} \text{ L} \cdot \text{mol}^{-1} \cdot \text{s}^{-1}$ ($n=3$, relative coefficient $R > 0.99$), indicating that quercitrin and CNAa form a stable complex. We then plotted a regression line based on Equation (2) (Figure 7f), and calculated $K_A = (2.30 \pm 0.43) \times 10^7 \text{ L} \cdot \text{mol}^{-1}$ and the number of binding sites to be $n = (1.45 \pm 0.08)$ ($R > 0.99$). These data indicate that the binding stoichiometry of quercitrin: CNAa was also about 1 : 1, and the binding of quercitrin to CNAa was stronger than to CNA.

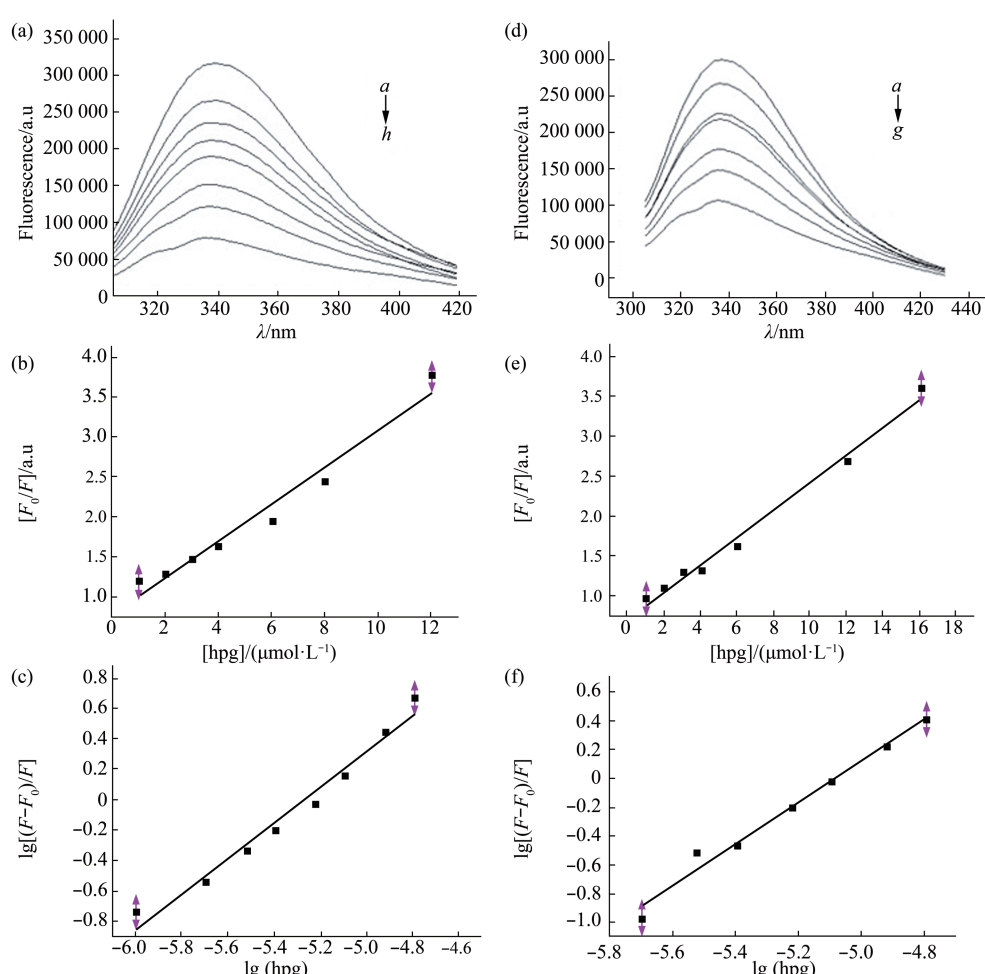


Fig. 7 Fluorescence spectra of CNA and CNAa in presence of quercitrin

(a) CNA fluorescence emission in the presence of quercitrin. Molar ratios of drug to protein were 0, 1, 1.5, 2, 3, 4, 6, 8 (from *a* to *h*) with 2 μmol/L CNA. (b) Stern-Volmer plots for the CNA-quercitrin system. (c) Plots of $\lg [(F_0 - F)/F]$ versus $\lg[Q]$ for the CNA-quercitrin system. (d) CNAa fluorescence emission in the presence of quercitrin. Molar ratio of drug to protein were 0, 2, 3, 4, 6, 8, 12 (from *a* to *g*) with 2 μmol/L CNAa. (e) Stern-Volmer plots for the CNAa-quercitrin system. (f) Plots of $\lg [(F_0 - F)/F]$ versus $\lg[Q]$ for the CNAa-quercitrin system. $\lambda_{\text{ex}} = 295 \text{ nm}$, in buffer containing 0.05 mol/L Tris-HCl with 2% (v/v) DMSO at pH 7.4.

2.10 Possible sites of binding of quercitrin to CN in catalytic domain identified by docking analysis

We calculated 35 results, which could be ranked in 7 groups, generated by Autodock 4. There were two high-ranked docking positions of quercitrin on CN,

which were coherent with the fluorescence results. Their free energy of binding were -6.35 kcal/mol (site 1) and -5.50 kcal/mol (site 2) (Figure 8a). The actual amino acid residues in simulations of site 1 were Pro340, Trp342, Tyr124 (Figure 8b); and of site 2 Lys52, Ala48, Pro338 (Figure 8c).

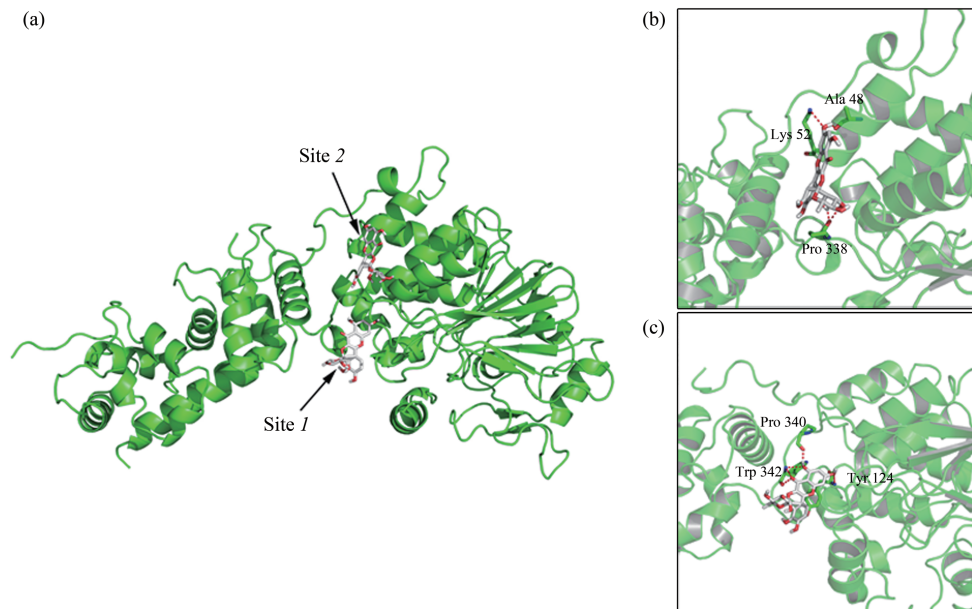


Fig. 8 Docking of quercitrin to CN

(a) Overall view of the docking between quercitrin and CN. (b) Site 1 with a free binding energy of -6.35 kcal/mol. (c) Site 2 with a free binding energy of -5.50 kcal/mol. Quercitrin is indicated by the sticks.

3 Discussion

CsA and FK506 are widely used as immunosuppressants in organ transplantation as well as in the treatment of autoimmune disorders^[36] in spite of side effects on liver, kidney, nervous system and other problems^[14]. In our search for alternative immunosuppressants we extracted flavonoids, the main component of the silk tree flower, and obtained quercitrin, which is the major flavonoid in these flowers. Quercitrin has been reported to be an antioxidant^[37], anti-inflammatory^[24-25], to regulate the autoimmune response^[26-27] and to induce apoptosis^[38]. It is also an inhibitor of Sortase A^[23]. It is first reported to inhibit CN activity with both p-NPP and ³²P-RII peptide as substrate, unlike CsA and FK506^[39].

Because of the important role of CN in immune regulation, we investigated the effect of quercitrin on immune reactions. Quercitrin was active in the mouse

spleen lymphocytes proliferation assay, in responses to the T lymphocyte mitogen Con A, and the B lymphocyte mitogen LPS. It also inhibited the MLR in mice. Inhibition of the MLR was stronger than of T cell and B cell proliferation. Given the critical role that CN plays in T lymphocyte activation, we presume that quercitrin exerts its immunosuppressive effect by inhibiting CN activity *in vivo*.

DTH is a reaction in which a specific antigen activates T lymphocytes to release cytokines^[40]. In our experiments, quercitrin alleviated paw edema in a dose-dependent manner in mice, which pointed to a suppressive effect on T cell-dependent immune responses. Quercitrin had the same effect as CsA at 40 mg/kg. In the DTH test described above, we observed that the mice of the CsA group displayed fur ruffling and emaciation, which were not seen in the quercitrin-treated group, suggesting that quercitrin has lower toxicity than CsA. The toxic side effects of

conventional medicine have received much attention in the last few years, with the result that more medicinal plants and their derivatives are being used as therapeutic alternatives^[41]. At present, CsA and FK506 are still widely used as immunosuppressants, but their long term side effects on liver, kidney and nerve^[42-44] are a serious disadvantage. Therefore, novel immunosuppressants with low toxicity and few side effects are greatly needed. In this study, we performed an acute toxicity test in mice with quercitrin, and used two different routes of administration, intraperitoneal injection and oral gavage. No mice died or exhibited abnormal reactions at doses of 2 000 mg/kg (*i.p.*) and 5 000 mg/kg (*i.g.*) during the experiment, which indicates that the LD_{50} is above 2 000 mg/kg with intraperitoneal injection and above 5 000 mg/kg with oral gavage. So we can consider quercitrin to have no or minimal toxicity. CsA has severe hepatotoxicity and nephrotoxicity, and can cause transaminase and total bilirubin levels to increase^[45]. Therefore we measured some specific biochemical indexes of liver and kidney function. The results of blood biochemistry showed that levels of serum creatinine, urea nitrogen, total bilirubin, alkaline phosphatase, glutamic-oxaloacetic transaminase, glutamic-pyruvic transaminase increased in mice receiving large intraperitoneal injections of CsA, but not in mice treated with quercitrin. Our previous study of quercitrin treatment of systemic lupus erythematosus in mice also showed that quercitrin had lower toxicity than CsA as long-term medication^[26]. Overall, quercitrin had less toxic side effects on experimental animals than CsA, and this advantage may become more obvious in long-term treatment.

Because CN controls T cell activity and other immune-related activities *via* the CN-NFAT signaling pathway, we examined the relationship of quercitrin to the CN-NFAT pathway in Jurkat cells and confirmed that quercitrin regulates T cells and immune activities by modulating CN-NFAT signaling pathway as CsA does.

In our previous study, quercitrin inhibited CN activity with both substrates, unlike CsA and FK506 did. This suggested that quercitrin bound directly to CN. To explore the interaction between quercitrin and CN we used fluorescence spectroscopy and docking. Quercitrin caused fluorescence quenching of CNA, the stoichiometry of quercitrin and CNA was 1 : 1

and the binding constant K_A was $(1.60 \pm 0.40) \times 10^6 \text{ L} \cdot \text{mol}^{-1}$, indicating strong binding. Quercitrin bound even more strongly to CNAa. It thus seems likely from all our results that quercitrin binds directly to the catalytic domain of CNA. To further explore the possible binding area of quercitrin with CN, we calculated each Trp-quercitrin distances by energy transfer experiments, and generated possible concrete binding sites for quercitrin in quercitrin-CN complex by Autodock 4 (Figure 8b, c), which all located in the catalytic domain of CNA but not the catalytic center^[5]. Additionally, Figure 7a shows that there was a slight blue shift of the maximum emission wavelength in the presence of quercitrin, which indicates protein secondary structure may change. Our study on CD spectra of CNA with quercitrin, which was in **Supplementary data**, showed a much tighter structure of the enzyme in presence of quercitrin.

In conclusion, our data indicate that quercitrin is a CN inhibitor of low toxicity that acts as an immunosuppressant by inhibiting the CN-NFAT signaling pathway. Unlike CsA and FK506, it binds directly to the catalytic domain of CN. It may be a useful new immunosuppressive agent.

4 Conclusion

We used CN as the target enzyme to explore the inhibitory effect of natural compound quercitrin and its possible mechanism of action. Quercitrin inhibited CN activity both *in vitro* and in intact cells, and also had good performance in reducing splenocyte proliferation and improving DTH symptoms in mice. The results of toxicological study showed that quercitrin had no or minimal toxic side effects on experimental animals. Fluorescence spectroscopy and molecular docking analysis showed that quercitrin may bind to two sites on the CN and participate in the regulation of immune response through the CN-NFAT pathway. In summary, we identified a new CN inhibitor, quercitrin, which could be a useful novel immunosuppressant with low toxicity.

Supplementary material PIBB_20210381_Doc_S1.pdf is available online (<http://www.pibb.ac.cn> or <http://www.cnki.net>).

References

- [1] Sieber M, Baumgrass R. Novel inhibitors of the calcineurin/

- NFATc hub-alternatives to CsA and FK506? *Cell Commun Signal*, 2009, **7**: 25
- [2] Lake J R, Gorman K J, Esquivel C O, et al. The impact of immunosuppressive regimens on the cost of liver transplantation—results from the US FK506 multicenter trial. *Transplantation*, 1995, **60**(10): 1089-1095
- [3] Sollinger H. Mycophenolate mofetil for the prevention of acute rejection in primary cadaveric renal allograft recipients. *Transplantation*, 1995, **60**(3): 225-232
- [4] Liu J, Farmer J D, Lane W S, et al. Calcineurin is a common target of cyclophilin-cyclosporin A and FKBP-FK506 complexes. *Cell*, 1991, **66**(4): 807-815
- [5] Rusnak F, Mertz P. Calcineurin: form and function. *Physiol Rev*, 2000, **80**(4): 1483
- [6] Li H, Rao A, Hogan P G. Interaction of calcineurin with substrates and targeting proteins. *Trends Cell Bio*, 2011, **21**(2): 91-103
- [7] Mass E, Wachten D, Aschenbrenner A C, et al. Murine Creld1 controls cardiac development through activation of calcineurin/NFATc1 signaling. *Dev Cell*, 2014, **28**(6): 711-726
- [8] Im S H, Rao A. Activation and deactivation of gene expression by Ca²⁺/calcineurin-NFAT-mediated signaling. *Mol Cells*, 2004, **18**(1): 1-9
- [9] Baksh S, Burakoff S J. The role of calcineurin in lymphocyte activation. *Semin Immunol*, 2000, **12**(4): 405-415
- [10] Jørgensen K A, Koefoed-Nielsen P, Karamperis N. Calcineurin phosphatase activity and immunosuppression. A review on the role of calcineurin phosphatase activity and the immunosuppressive effect of cyclosporin A and tacrolimus. *Scand J Immunol*, 2003, **57**(2): 93-98
- [11] Fedele A O, Carraro V, Xie J, et al. Cyclosporin A but not FK506 activates the integrated stress response in human cells. *J Biol Chem*, 2020, **295**(44): 15134-15143
- [12] Mika A, Stepnowski P. Current methods of the analysis of immunosuppressive agents in clinical materials: a review. *J Pharmaceut Biomed*, 2016, **127**: 207-231
- [13] Feutren G, Mihatsch M J. Risk factors for cyclosporine-induced nephropathy in patients with autoimmune diseases. *New Engl J Med*, 1992, **326**(25): 1654-1660
- [14] Hong J C, Kahan B D. Immunosuppressive agents in organ transplantation: past, present, and future. *Semin Nephrol*, 2000, **20**(2): 108-125
- [15] Cen J, Shi M, Yang Y, et al. Isogarcinol is a new immunosuppressant. *PLoS One*, 2013, **8**(6): e66503
- [16] Wang H, Zhou C L, Lei H, et al. Inhibition of calcineurin by quercetin *in vitro* and in Jurkat cells. *J Biochem*, 2010, **147**(2): 185-190
- [17] Li J, Tu Y, Tong L, et al. Immunosuppressive activity on the murine immune responses of glycyrol from Glycyrrhiza uralensis via inhibition of calcineurin activity. *Pharm Biol*, 2010, **48**(10): 1177-1184
- [18] Kang T, Jeong S, Kim N, et al. Sedative activity of two flavonol glycosides isolated from the flowers of *Albizia julibrissin* Durazz. *J Ethnopharmacol*, 2000, **71**(1): 321-323
- [19] Yahagi T, Daikonya A, Kitanaka S. Flavonol acylglycosides from flower of *Albizia julibrissin* and their inhibitory effects on lipid accumulation in 3T3-L1 cells. *Chem Pharm Bull*, 2012, **60**(1): 129-136
- [20] 中华人民共和国卫生部药典委员会. 中华人民共和国药典. 北京: 人民卫生出版社, 1977: 260
- Pharmacopoeia Committee of the Ministry of Health. Pharmacopoeia of the People's Republic of China. Beijing: People's medical publishing house, 1977: 260
- [21] Sun H, He S, Shi M. Adjuvant-active fraction from *Albizia julibrissin* saponins improves immune responses by inducing cytokine and chemokine at the site of injection. *Int Immunopharmacol*, 2014, **22**(2): 346-355
- [22] Kim J J, Lee B E, Jung D S, et al. Immunoregulatory effects of extracts from the stem bark of *Albizia julibrissin* Durazz. *Int J Oral Bio*, 2004, **29**(4): 137-144
- [23] Liu B, Chen F, Bi C, et al. Quercitrin, an inhibitor of sortase A, interferes with the adhesion of *Staphylococcal aureus*. *Molecules*, 2015, **20**(4): 6533-6543
- [24] Comalada M, Camuesco D, Sierra S, et al. *In vivo* quercitrin anti-inflammatory effect involves release of quercetin, which inhibits inflammation through down-regulation of the NF-κB pathway. *Eur J Immunol*, 2005, **35**(2): 584-592
- [25] Lee J H, Ahn J, Kim J W, et al. Flavonoids from the aerial parts of *Houttuynia cordata* attenuate lung inflammation in mice. *Arch Pharm Res*, 2015, **38**(7): 1304-1311
- [26] Li W, Li H, Zhang M, et al. Quercitrin ameliorates the development of systemic lupus erythematosus-like disease in a chronic graft-versus-host murine model. *Am J Physiol Renal Physiol*, 2016, **311**(1): F217-F226
- [27] Chen S, Li H, Liu Y, et al. Quercitrin extracted from Tartary buckwheat alleviates imiquimod-induced psoriasis-like dermatitis in mice by inhibiting the Th17 cell response. *J Funct Foods*, 2017, **38**: 9-19
- [28] Wang H L, Du Y W, Xiang B Q, et al. The regulatory domains of CNA have different effects on the inhibition of CN activity by FK506 and CsA. *IUBMB Life*, 2007, **59**(6): 388-393
- [29] Stallard N, Whitehead A. Reducing animal numbers in the fixed-dose procedure. *Hum Exp Toxicol*, 1995, **14**(4): 315-323
- [30] Nan Y, Wang R, Yuan L, et al. Effects of *Lycium barbarum* polysaccharides (LBP) on immune function of mice. *Afr J Microbiol Res*, 2012, **6**(22): 4757-4760
- [31] Lei H, Qi Y, Jia Z G, et al. Studies on the interactions of kaempferol to calcineurin by spectroscopic methods and docking. *BBA-Proteins Proteom*, 2009, **1794**(8): 1269-1275
- [32] Kang J, Liu Y, Xie M X, et al. Interactions of human serum albumin with chlorogenic acid and ferulic acid. *BBA-Gen Subjects*, 2004, **1674**(2): 205-214
- [33] Eftink M R. Fluorescence quenching reactions. *Biophysical and biochemical aspects of fluorescence spectroscopy*. New York: Plenum Press, 1991

- [34] Yasir M, Sultana B, Nigam P S, et al. Antioxidant and genoprotective activity of selected cucurbitaceae seed extracts and LC-ESIMS/MS identification of phenolic components. *Food Chem*, 2016, **199**: 307-313
- [35] Wiederrecht G, Lam E, Hung S, et al. The mechanism of action of FK-506 and cyclosporin A. *Ann NY Acad Sci*, 1993, **696**(1): 9-19
- [36] Guada M, Sebastián V, Irusta S, et al. Lipid nanoparticles for cyclosporine A administration: development, characterization, and *in vitro* evaluation of their immunosuppression activity. *Int J Nanomed*, 2015, **10**6541
- [37] Zakaria Z A, Balan T, Mamat S S, et al. Mechanisms of gastroprotection of methanol extract of *Melastoma malabathricum* leaves. *BMC Complement Altern Med*, 2015, **15**(1): 1
- [38] Dai X, Ding Y, Zhang Z, et al. Quercetin and quercitrin protect against cytokine-induced injuries in RINm5F β -cells via the mitochondrial pathway and NF- κ B signaling. *Int J Mol Med*, 2013, **31**(1): 265-271
- [39] Takai A, Mieskes G. Inhibitory effect of okadaic acid on the p-nitrophenyl phosphate phosphatase activity of protein phosphatases. *Biochem J*, 1991, **275**(1): 233-239
- [40] Elgert K D. Immunology: understanding the immune system. New York: Wiley-Liss, 1996: 788-789
- [41] Salem M L. Immunomodulatory and therapeutic properties of the *Nigella sativa* L. seed. *Int Immunopharmacol*, 2005, **5**(13): 1749-1770
- [42] Shaw L, Kaplan B, Kaufman D. Toxic effects of immunosuppressive drugs: mechanisms and strategies for controlling them. *Clin Chem*, 1996, **42**(8): 1316-1321
- [43] El-Sherbeeny N A, Nader M A. The protective effect of vildagliptin in chronic experimental cyclosporine A-induced hepatotoxicity. *Can J Physiol Pharm*, 2015, **94**(999): 1-6
- [44] Ateyya H. Amelioration of cyclosporine induced nephrotoxicity by dipeptidyl peptidase inhibitor vildagliptin. *Int Immunopharmacol*, 2015, **28**(1): 571-577
- [45] Bennett W M, Norman D J. Action and toxicity of cyclosporine. *Annu Rev Med*, 1986, **37**(1): 215-224

槲皮苷：一种抑制钙调蛋白磷酸酶(CN)的新型免疫抑制剂*

王梦奇^{1,2)**} 柳继琼^{1)**} 佟丽^{1)**} 谢雨菲^{1,3)} 陈晖¹⁾ 赵长云¹⁾

王磊¹⁾ 刘媛媛¹⁾ 高雅丹¹⁾ 张牧¹⁾ 向本琼^{1)***} 魏群^{1)***}

(¹) 北京师范大学生命科学学院, 北京市基因工程药物及生物技术重点实验室, 北京 100875;

(²) 北京师范大学出版社, 北京 100088; (³) 长沙理工大学化学与食品工程学院, 长沙 410114)

摘要 目的 以钙调蛋白磷酸酶(CN)为靶酶, 从中草药中寻找高效、低毒的免疫抑制剂。方法 以CN为靶点, 筛选并分离能够抑制其活性的天然化合物。在细胞和动物水平评价该化合物的免疫抑制效果及毒副作用, 并通过荧光猝灭、分子对接、免疫印迹、双荧光素酶报告基因、实时定量PCR等实验探究天然化合物与CN的作用机理及可能的免疫抑制作用机制。结果 槲皮苷在体外和细胞内均能抑制CN的活性, 并且能够有效抑制小鼠脾细胞的增殖, 缓解小鼠迟发超敏反应。毒理研究结果显示, 槲皮苷对实验小鼠无急性毒性, 且毒副作用很小。荧光猝灭实验和分子对接分析表明, 槲皮苷可能与CN上的两个位点相结合, 并通过CN-NFAT通路参与调节免疫反应。结论 通过筛选获得了新型CN抑制剂槲皮苷。槲皮苷具有成为新型低毒免疫抑制剂的潜在可能。

关键词 槲皮苷, 钙调神经磷酸酶, 免疫, CN-NFAT信号通路, 相互作用

中图分类号 Q2, Q5

DOI: 10.16476/j.pibb.2021.0381

* 国家自然科学基金(30970636)资助项目。

** 并列第一作者。

*** 通讯联系人。

魏群 Tel: 010-58807365, E-mail: weiq@bnu.edu.cn

向本琼 Tel: 010-58807221, E-mail: xiangbq@bnu.edu.cn

收稿日期: 2021-12-08, 接受日期: 2021-12-25